Vol. 40, No. 4 (2018) 654-669, DOI: 10.24874/ti.2018.40.04.12

Tribology in Industry

www.tribology.rs

RESEARCH

Influence of Binder on Thermomechanical and Tribological Performance in Brake Pad

B.S. Rajan[a], M.A.S. Balaji[a], K. Sathickbasha[a], P. Hariharasakthisudan[b]

[a] *Department of Mechanical Engineering, B S Abdur Rahman Crescent Institute of Science and Technology, Vandalur, Chennai, India,*
[b] *Department of Mechanical Engineering, National Engineering College Kovilpatti, Tamil Nadu, India.*

Keywords:

Brakes
Friction Mechanisms
Friction Test Methods
Thermal Stability
TGA
Polymers (solid)
Wear Mechanisms

Corresponding author:

B.S. Rajan
Department of Mechanical Engineering, B S Abdur Rahman Crescent Institute of Science and Technology, Vandalur, Chennai, India.
E-mail: suryarajan.b@gmail.com

A B S T R A C T

The type of binder and its fraction in the brake pad material formulation plays a vital role in fulfilling the key requirements of friction materials (FMs). Three set of brake pads were fabricated with 10, 12 and 14 weight percentage (wt%) of Epoxy-Modified novalac Phenolic (EMP) resin and designated as DB10, DB12, and DB14 respectively. The characterization of resin and composites were done using standard techniques. The tribological tests were carried out on an Inertia Brake Dynamometer (IBD) following industry standards JASO C-406 and JASO C-427. The friction and wear behavior based on the rotor temperature, rotor speed, and pad pressure was analyzed. It was observed that DB10 showed 12.8 % more thermal stability, 37.01 % more fade resistance and 11.54 % improved recovery rate than DB14. DB14 showed high wear resistance at 100, 200 and 300 °C for the speed of 50 km/h.

1. INTRODUCTION

The brake pad is a component of a disc brake system used in automotive. The function of the brake pad is to convert the kinetic energy of the vehicle into frictional heat energy through sliding action with the rotor in the vehicle. The material of the brake pad generally comprises five constituents such as filler, fiber, abrasive, lubricant and binder [1]. The function of the binder among these constituents plays a vital role in deciding the performance of the brake pad. Binders ensure the structural integrity of the composite in the applications of the brake pad. Several binders such as phenolic, phenolic modified Cashew Nut Shell Liquid (CNSL), rubber and cardanol are used in brake pad materials. Among all the binders, phenolic binder (novolac) exhibited superior frictional properties even at high temperature 350 – 420 °C [2]. The capacity of binders is defined based thermal stability and oxidation resistance at elevated temperature.

In passenger cars, the maximum temperature rise of the rotor and disc pads is up to 400 °C. The Coefficient of Friction (CoF) of the brake pad reduces when brake pads exposed to such high

temperature for an extended period; this phenomenon termed fade. The load, speed and high temperature at the interface are identified as the significant factors responsible for the fade of the brake pad [3]. The organic ingredients and few inorganic materials in the brake pad material also influenced by the fade phenomena [4,5].

It is inevitable to choose a binder for Friction Composites (FCs) with high thermal stability at elevated temperature to control the fade phenomena [6]. The type and quantity of binder in the brake pad material formulation play a critical role to manage the fade resistance of the brake pad material [7,8]. The optimum quantity of binder yields structural integrity to the brake pad without sacrificing other significant properties [1]. These research works were conducted by modifying the resin and improving the molecular weight of the resin to enhance the friction and wear resistance of the brake pad material. Seong Jin Kim et al. have identified that the modified resin showed superior friction stability and wear resistance than straight resin [9]. The phenolic resin was modified with Si and Boron phosphorous individually and studied for its fade resistance and wear resistance. It observed that Boron phosphorous modified phenolic resin revealed better results than straight phenolic resin [10]. Similarly, CSNL modified with orthophosphoric acid, and neat CSNL tested for fade and recovery. It is proved that the modified version improved the fade and wear resistance [11]. J Bijwe et al. reported that the trends in performance properties of brake pad materials were not changing uniformly with increasing content of binder[8]. The influence of altering the molecular weight of Alkylbenzene modified resin on a disc brake pad was investigated and found that the medium molecular weight reduced the fluctuations of CoF [12]. The research works were commonly conducted on a different type of resins, modified resins with fillers. The composites prepared in most of the research work tested for wear conditions using small sample testing machines like pin-on-disc, pad-on-disc, FAST, Chase, Krauss and other indigenously developed Tribometer. Tsang et al. [11] emphasized that the tests conducted using small sample testing machine have not identified as promising test methods for screening automotive brake pads. This was due to the large variability in friction results observed in the small size testing machines [12]. Very few works reported on the influence of the binder quantity and evaluation in more rigorous conditions using an IBD.

In the present work, Epoxy Modified Phenolic (EMP) resin selected because of its good thermomechanical properties and wetting ability with other ingredients in the formulation. This research work aims to study the effect of weight (wt) % of the EMP resin in the brake pad material. Three sets of brake friction composites, with the same parent formulation and different wt% of the EMP resin, were fabricated to evaluate the friction and wear performance. Various tests carried out to investigate the physical, chemical, mechanical, and tribological properties as per standards used in the automotive industries. Thermal stability of the brake pad was checked by Thermogravimetric Analysis (TGA) / Differential Thermal Analysis (DTA) and Differential Scanning Calorimeter (DSC). Friction tests were carried out on an IBD as per test standard JASO C-406, and the wear test conducted following standard JASO C-427. Scanning Electron Microscopy (SEM) analysis was performed on the worn out surface to know the wear mechanism.

2. MATERIALS

EMP resin procured from M/s. Esterkote chemicals Chennai, India. TGA/DTA of the resin was carried out in the Jupiter simultaneous thermal analyzer (Model STA 449 F3, NETZSCH, and Germany). The resin was heated in the alumina pans (5-10 mg) under air atmosphere. The rate of heating was maintained at 10 °C/min.

Table 1. Properties of the EMP resin.

Properties	**Epoxy modified phenolic resin**
Melting point	84 ˚C
Gel Time at 150˚C (ISO 8987 B)	67 – 110 sec
Flow length test at 135 ˚C (ISO 8619)	62 mm
Hexa content	10 %
Moisture content	2.1 %

The DSC analysis conducted in a thermal analyzer (TA-60 WS), with the temperature rate

of 10 °C/min. The DSC system was kept nitrogen atmosphere with a flow rate of 20 ml/min. The mass of 10 mg was placed in a closed aluminum sample chamber to obtain the thermo-reaction behaviour. The resin also characterized for flow distance, melting point, Gel Time, flow length, Hexa & moisture content (%) by standard methods. The results displayed in Table 1.

2.1 Thermogravimetric Analysis

TG analysis of the EMP resin illustrated two stages of weight loss as shown in Fig. 1. The resin exhibited a weight loss of 5 % up to 380 °C in the stage-1.

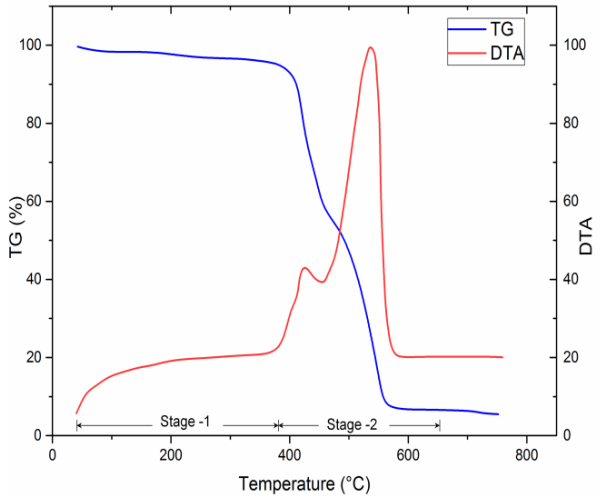

Fig. 1. Thermal Gravimetric Analysis of resin.

In the stage-2 of TGA/DTA at 380-650 °C, the weight loss was 89 %, and this maximum weight loss is due to the thermo-oxidative reactions, leaving a carbon residue equal to 6 % of the initial mass. From the TGA results, it was identified that the resin started to decompose above 360 °C.

2.2 DSC Analysis

DSC test is a promising technique to obtain the thermal profile of the material under the conditions of thermal dynamic (linear temperature ramp) scanning. The reaction behavior of the material from the room temperature to 200 °C was obtained from this test. The DSC curve of the EMP resin depicted in figure 2. The reaction started at around 150 °C, and reached the peak at 156 °C, and ended at 173 °C. The curing temperature of the resin finalized as 156 °C from this result.

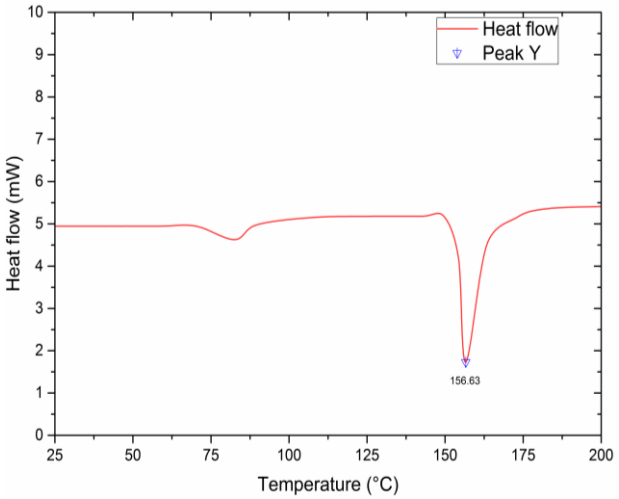

Fig. 2. The result of the DSC analysis.

2.3 Fabrication of brake pad

The brake pads are fabricated in four steps process, which are mixing of ingredients, preforming, curing and post-baking. The formulation of the brake pad materials was carried out by keeping all other ingredients at constant wt% except the resin and the Baryte. The variation in resin and Baryte of all the three brake pads shown in Table 2. In one of the author's previous work, the content of two organic material namely Phenolic resin and organic friction dust in the formulation was studied [13]. The variation of organic content in the study is 4 wt%, which cause a major difference in the tribological study. Based on this study, the total organic content variation in this study is taken as 4 wt% and the resin content in the brake pad taken as 10, 12 and 14 wt%.

Table 2. Variation of binder content in brake pads.

Ingredients	Brake pads		
	DB10	DB12	DB14
EMP resin (wt. %)	10	12	14
Barytes (wt. %)	10	8	6
Other ingredient (wt. %)	80	80	80

The other ingredients (wt%)in the formulation were Kevlar (1.8 %), cellulose fiber (1.2 %), Rockwool fiber (12 %), copper fiber (8 %), steel wool (12.5 %), green chrome oxide (3 %), graphite powder (10 %), crumb rubber (1 %), rubber NBR (1 %), friction dust (7.5 %), china clay (17 %) and magnesium oxide (5 %). These additional ingredients were mixed in a shear mixer with feeder and chopper. The homogeneous mixture was then introduced into a two- cavity mold

supported with the shot peened and adhesive coated steel back plates. The composites in the form of pads were molded in a hydraulic press [14]. The different steps in the fabrication of composite are shown in Fig. 3.

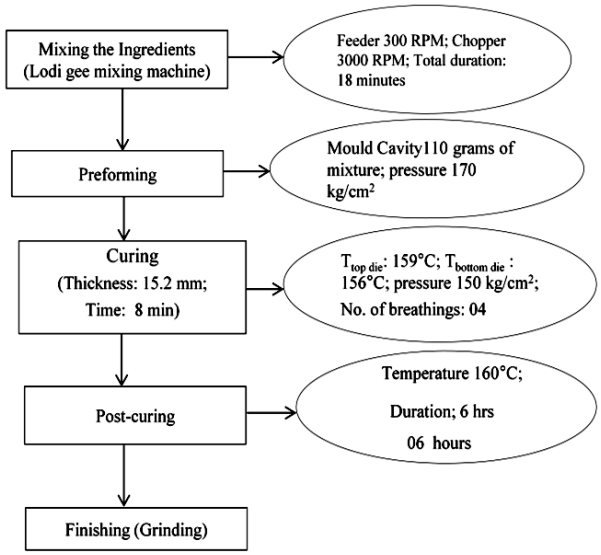

Fig.3. Fabrication Process of brake pads.

The FM ingredients added in the following sequence during mixing (in the Lodigi shear mixing machine).

a) Reinforcing fibers and pulp ingredients (06 minutes)

b) Powder ingredients (08 minutes)

c) Binder (04 minutes)

3. EXPERIMENTAL METHODS

3.1 Friction test

In the present work, the friction test was conducted using IBD. The test was conducted by following industry standard JASO C-406 which is used for determining the CoF of brake pads used in the passenger car. The friction test schedule is given in Table 3. Bedding was done at 120 °C to establish the conformal contact between the mating surfaces. The friction tests were carried out at three braking speeds, such as 50, 100 and 130 km/h. The tests carried out with different decelerations from 0.1 to 0.8 g. The brake rotor deceleration was controlled by braking pressure, which was programmed to achieve a selected rate of deceleration. The applied pressure and speed are essential parameters during braking as the μ is dependent on it. The variation in μ is expected to be as low as possible. The tribological test performed on a double-ended full-scale IBD, and the schematic diagram as shown in Fig. 4. The specification of the IBD and test conditions are given in Table 4.

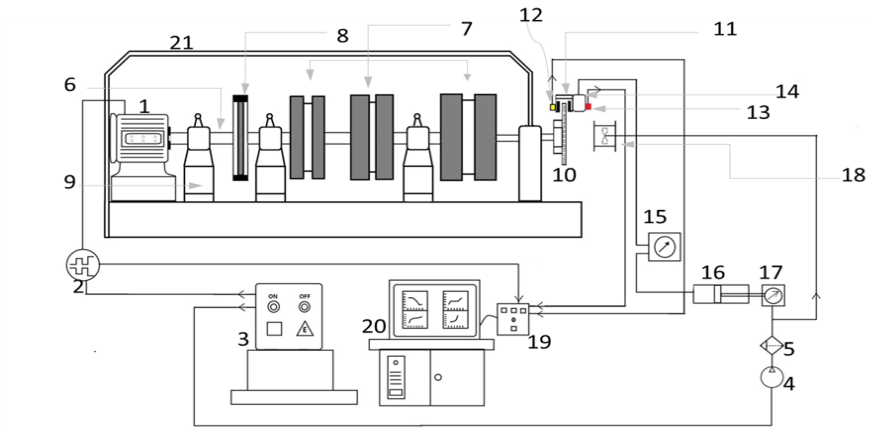

Fig. 4. Schematic diagram of Double ended full-scale IBD.

1. D.C Motor	8. Emergency Brake	15. Hydraulic Pressure sensor
2. Encoder	9. Bearings	16. Hydraulic piston cylinder
3. A.C Power supply	10. Rotor Disc	17. Pneumatic Pressure sensor
4. Air Compressor	11. Caliper	18. Blower
5. Air Filter	12. Thermocouple	19. Data Acquisition system
6. Main shaft	13. Torque sensor	20. Monitor output
7. Inertia Wheels	14. Brake fluid Receptacle	21. Outer cover

Table 3. Friction test schedule based on JASO 406.

Effectiveness Test					
Procedure	**Speed (Km/h)**	**Brake deceleration m/s²**	**Initial brake temperature ˚C**	**No. of applications**	**Air Blower**
Burnish/Bedding	50	0.1 g to 0.8g	120	200	ON
Effectiveness I	50,100	0.1 g to 0.8g	80	16	ON
Effectiveness II	50,100,130	0.1 g to 0.8g	<80	24	ON
Effectiveness III	50,100,130	0.1 g to 0.8g	<100	24	ON
Fade & Recovery-I					
Fade cycles	100	3 & 4	90 ˚C for 1st break	10	OFF
Recovery cycles	100	3 & 4	>80 ˚C	10	ON

Table 4. Friction test conditions

Detail	Specification
Standard	JASO C-406
Brake assembly model	PE54C-14
Inertial Load	49 kg-ms²
Rolling or tire radius	0.293 m
Effective radius (pad on disc sliding radius)	0.103 m
The thickness of the pad along with the back plate	15.2 mm

3.2 Wear Test

The wear behavior of the developed brake pad was tested using the IBD. The test was conducted by following the standard JASO C-427. In this testing method, the wear rate of both pad and rotor disc was calculated over the temperature range of 100 °C to 300 °C for 500 to 1000 brake applications. The temperature was measured on the rotating disc, precisely in the middle of the effective contact area, with the help of contact type of thermocouple. The cooling wind at the velocity of 11 m/s was blown uniformly on the braking device to simulate the real vehicle running condition for the test setup. The wear thickness loss was measured and tabulated after a specific number of applications of brake at a specific temperature (100 °C, 200 °C, 250 °C and 300 °C).

The burnishing cycle run at the speed of 50 km/h, for 200 brake applications. The temperature during burnishing cycle measured as 100 °C which confirmed the definite contact between the disc and the pad. The wear test started with a measurement of the initial thickness of the brake pad at 8 different positions. Wear test-I conducted for 1000 brake applications with initial temperatures of disc raised to 100, 200, and 250 °C. The steps involved in the schedule displayed in Table 5.

3.3 Mechanical Tests

The specific gravity of the developed composites was identified by the water displacement method. Hardness test was conducted in a Rockwell testing machine using 'S' scale. The average value of five indentations was made from the center to the edge of the specimen to obtain the proper hardness for each developed brake FC. The shear strength indicates the bonding strength of the FM with the back plate. It was determined using ISO 6312 standards. The cold shear strength test was conducted at the ambient temperature, and the hot shear strength held after heating the composite to 200 °C. The porosity of the FM evaluated following JIS D 4418 (1996) standards.

Table 5. Wear test schedule.

Step	Test Conditions	Initial Speed km/h	Disc Temperature	Number of brake applications at a deceleration of 0.3(g) m/s²
1	Burnish/Bedding	50	100°C	200
2	Wear test-I	50	100°C, 200°C, 250°C and 300°C	1000 - (100°C to 250°C) 500 - (300°C)
3	Wear test-II	50	100°C and 200°C	500
4	High Speed Wear test (HS)	100	100°C	100

4. RESULTS AND DISCUSSION

4.1 Effect of the resin content on mechanical and thermal properties of brake pads

The specific gravity and the hardness of the brake pad decreased when the resin content in the material formulation increased. The reduction in specific gravity of pads may be due to the removal of baryte (to compensate resin) which possessed a higher specific gravity [15]. Similarly, the reduction of hardness is also due to the removal of hard barite particle and the inclusion of additional soft binder. The increase of resin content helped to strengthen the interfacial bonding between the reinforced fibers and the resin matrix. The increment in interfacial bonding improved the shear strength of the brake pad material. The results were shown in Table 6.

Table 6. Physical and mechanical properties of the brake pads.

Properties	Unit	DB10	DB12	DB14
Specific gravity	-	2.72	2.55	2.46
Hardness	HR 'S'	102	98	90
Cold Shear Strength	Kg/cm²	41.70	42.12	43.09
Hot Shear Strength	Kg/cm²	25.48	26.0	25.67
Porosity	%	19	18	16

Porosity plays a vital role in the mechanical and thermal properties of the FMs. H Jang et al. [16] expressed that the size and distribution of internal pores affect the thermal conductivity of the composite. The porosity decreased with the increasing resin content. The fluidity of the resin may predict this through gaps inside the FM during hot pressing. The resin filled the voids before it was consolidated during curing.

The TGA results of the three brake pads shown in figure 5. It expressed the percentage of weight loss and the degradation temperature when the composites exposed to 800 °C from ambient temperature. The TG curves of three composites showed a two-stage mass loss, which was denoted by two peaks in the DTA curve. The minor degradation (Stage-I) was noted during 260-390 °C, and the major (Stage-II) decomposition rate started at approximately 390 °C and ends at 640 °C. The first stage mass (first smaller peak of TG/DTA represents the first stage mass loss) loss may be due to the low thermal resistive organic components than the binder namely, crumb rubber and cellulose fibers in the formulation. These ingredients cause early degradation of brake pad than the pure resin content [17]. Even though they provoked a little early degradation of the composite, Cellulose fiber is essential in the formulation to get the strength of the preform and the crumb rubber is vital to get the damping effect in the brake pads.

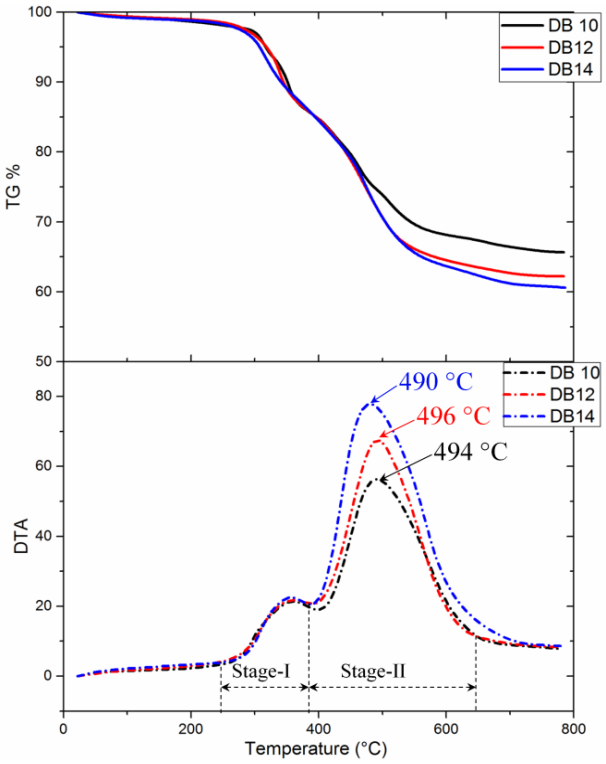

Fig. 5. TGA/DTA results.

This phenomenon might have happened due to cracking and dehydrogenation. The second stage mass loss was predicted by the degradation of the organic binder followed by forming a char [18,19]. GM Ingo et al. [18] observed and reported similar kinetics of materials. Bijwee et al. [15] highlighted similar effects and concluded that the deterioration of the binder in brake pads occurred during the operation at 300 – 400 °C. In this work, the second stage (second highest peak of TG/DTA represent the second stage mass loss) of degradation was observed between 390 – 640 °C. This showed the improved thermal stability of the brake pad composites. The content of EMP resin increased the thermal resistance of the composites and delayed the degradation process. This expressed

that the composite materials DB14 can be used in the temperature range upto 370 °C [20]. Hong et al. [10] examined the wear behavior of three varieties of resin. They found that the wear process relied on breakage of hydrogen bonding up to 200 °C and at temperatures higher than 300 °C. The resin went through random scission of polymer chains, oxidation, and carbonization. These results were in conformity with the results of the present study.

The weight loss % of the samples at degradation temperature was measured and shown in table 7. The considerable changes in weight were not observed in the first stage degradation temperature. The peaks of DTA were varied considerably as the resin content increased in the second stage-II.

Table 7. Degradation temperatures and corresponding weight loss of the brake pads in stage-II.

Designation	Degradation Temperature		Weight loss (%)	
	Stage-II		Stage-II	
	Start	End	Start	End
	T_1 (°C)	T_2 (°C)	W_1 (%)	W_2 (%)
DB10	398	640	15.75	34.33
DB12	396	640	15.64	37.79
DB14	394	640	15.88	39.39

Brake pad DB14 showed maximum weight-loss in the temperature range 394 to 640 °C. The DTA peak was observed at the temperature 490 °C which indicates the more thermal reactive nature (degradation) of the DB14 due to the high resin. The variation in the weight loss W_2 (%) shown in Table 7 was mainly attributed to the increase in the resin content of formulation as the other ingredients of the brake pad material kept constant. This inference was supported by Jie Fei et al. [21] who studied the effect of resin content by developing paper-based FM. They reported that the thermal stability of the FMs decreased with the increment in resin content.

4.2 Effect of the resin content on the frictional performance of brake pad

The friction test results are shown in figure 6. The test conditions and test schedule were discussed in section 3.1. It was observed from the results that the CoF was high for all the composites at low speeds and at low pressure (deceleration). The average CoF of DB14 was slightly higher ($\bar{\mu}$DB14 = 0.41) than DB12 ($\bar{\mu}$DB12 = 0.39) and DB10 ($\bar{\mu}$DB10 = 0.37) at the speed of 50 km/h irrespective of deceleration. The standard error in the CoF of DB10, DB12 and DB14 friction composite is 6.82 %, 4.01 % and 4.20 % respectively. At 50 km/h, the increase in deceleration does not much affect the CoF. The interface temperature generated at 50 km/h is not sufficient to degrade the resin rapidly. It also inferred by the higher performance of DB14 at 50 km/h. The increase in pressure also indirectly intensify the real area of contact and subsequently escalate better adhesion and CoF. A similar observation was reported by Mikael Eriksson et al [22]. From the theory of tribology, the braking pressure or load influences the friction force by changing the real contact area of rubbing surfaces. The dependence of CoF (μ) can be understood using the basic relation (Eq-1) [23].

$$\mu = \frac{A_0 \tau}{pA} \quad (1)$$

Where 'A_0' represents the real area of contact, 'A' denotes the surface area of contact (pad), 'τ' indicates the shear strength of the adhered surface and 'p' represents the braking pressure.

It was also observed (from Fig. 6) that for higher speeds (100 and 130 km/h), the brake pads showed highest values of μ at low deceleration/pressure. This could be recognized by the fact that the load carrying elements on the friction surface operates safely well below their load limits [24]. The shear stress input was fully converted as frictional output. At high speed and high deceleration/pressure, μ tends to decrease (generally referred as pressure fade). The difference between the maximum and minimum CoF (Δμ) at 100 km/h in all three types of brake pads were calculated as $\Delta\mu_{(DB14)}$ = 0.02, $\Delta\mu_{(DB12)}$ = 0.02 and $\Delta\mu_{(DB10)}$ = 0.01. Due to the friction process, the interface materials like polymer matrix, rubber, and organic fiber melts. Because of high organic content and low thermal stability of DB14, the dry lubrication system turned into a mixed lubrication system with the semi-solid third body material on the friction surface. The rheological surface properties change more rapidly with thermodynamic action at the interface which reduced the shear strength of the contact film [25,26] and subsequently reduces the μ. Similarly, Δμ at 130 km/h effectiveness test for DB14, DB12 and DB10 where noted as 0.04, 0.05, and 0.03 respectively.

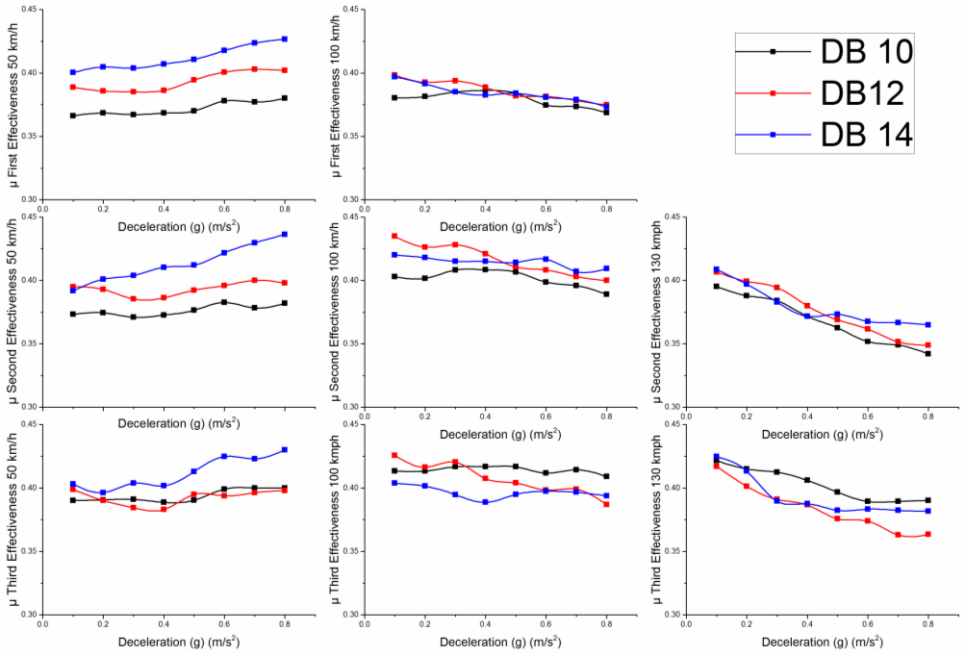

Fig. 6. Friction test results.

The above results indicate that DB14 and DB12 were more sensitive to deceleration whereas DB10 is less sensitive. The reason may attribute to the heat energy developed due to the increase in speed and pressure is high at the friction interface. Therefore the amount of material melts at the interface increases with high heat energy [27]. Therefore, the further increase in the speed increases the thickness of the semisolid film with a sliding action. So, the increased thickness in the interfacial semi-solid tribo layer reduces the CoF (Δμ) of 0.02 at 100 km/h and 0.05 at 130 km/h. The TGA results in Fig. 5 confirmed it. At higher temperatures, resin underwent for pyrolysis, and the gases such as CO_2 and CO were then released to form a gaseous layer above the transfer film surface. As a result, the friction pattern changed from dry friction to half lubricated with gases. PEI/MoS_2 ultra-thin film on steel substrate produced remarkably low friction coefficient in the N_2 gas atmosphere. The softening of resin at high temperature might be further complemented by the reduction in friction [28]. The DB14 and DB12 which possessed a high amount of resin degraded and produced more gases. These gases offered a resisting force to the applied load and thereby reduced the friction force [23].

4.3 Fade and recovery behavior

The fading condition of the brake is foreseen in downhill braking when the temperature at the interface goes beyond 450 °C, and fading friction becomes very significant. The brake pad materials were tested for fading friction by continuously applying brake for 10 stops. The fading cycle was planned for each brake application from 100 km/h to 0 km/h. It was represented in Fig. 7.

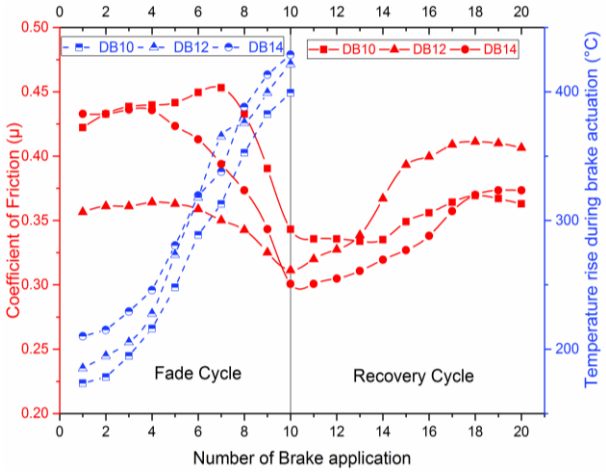

Fig. 7. Fade and recovery cycle.

The temperature of the interface was recorded as high as 400–450 °C. The initial increase in temperature up to 200 °C was obtained with the first 3 or 4 stops (Fig. 7). The temperatures falling in the range of 250 to 475 °C reported for the onset of the main transformations involved in the degradation of resin [29,30]. Figure 7 show that the CoF of DB14 dropped to 0.3 from 0.44 in 10 stops. The

fading started at the 5th stop. The corresponding disc temperature was equal to 273 °C. The CoF of DB12 declined from 0.36 to 0.31. The fading process begins at the 7th stop and the corresponding disc temperature observed at 315 °C. In the case of DB10, the average CoF reduced from 0.45 to 0.34. The fading started after the 8th stop. The corresponding disc temperature was equal to 338 °C. The rapid drop in COF considered undesirable. The fading resistance of DB10 was comparatively superior to other brake pads.

Among these three brake pads, DB14 exhibited early fading during the braking process.

It may be correlated with the poor thermal stability of the composite with high resin content as discussed in section 3.1.

μ_{fade} = lowest CoF recorded during the fade test

$$\%Fade\ rate = \frac{[\mu_{max} - \mu_{Fade}]}{\mu_{max}} \times 100 \quad (2)$$

Fading friction at any given speed with continuous braking is more critical and fading rate essentially is expected to be less than 25 % at temperatures as high as 300-450 °C. The % fade rate calculated through Eq-2 tabulated in Table 8. The composites DB10 and DB12 were observed to maintain a fade rate below the critical limit (i.e., 25 %). The brake pad DB14 showed the fade rate of 30.23 %. The thermal degradation of organic ingredients was observed as primary causes for fade due to the accumulation of heat in the interface [25]. The resin was an organic ingredient. The tribomechanical properties of the resin get changes above its glass transition temperature. The resin in the brake pad was exposed to excess heat during degradation and transformed into char, as discussed in our earlier sections. This transformation weakened the binding force and caused the changes in real contacts at the friction interface [31]. The resin content encouraged the fade rate as observed in the case of DB14.

A good recovery trend observed in all the developed composites after the fading cycles. The brake pad DB10 showed comparatively good recovery characteristics. The slow recovery rate considered undesirable behavior in brake pads.

Table 8. Fade and recovery properties of brake pads.

Test cycle	Parameters	DB10	DB12	DB14
Fade	μ-Fade	0.34	0.31	0.30
	% Fade rate	19.04	13.88	30.23
	Max. Disc temp (°C)	379	399	422
Recovery	μ-Recovery	0.36	0.41	0.37
	% Recovery rate	91.66	78.04	81.08

$\mu_{recovery}$ = highest CoF recorded during recovery test

$$\%Recovery\ rate = \frac{\mu_{min}}{\mu_{recovery}} \times 100 \quad (3)$$

In general, the recovery rate of the brake pad materials is expected to be in the range of 75–100 %. The recovery rate of all friction composites was calculated using Eq-3 and tabulated in Table 8. All the composites exhibited recovery rate within the acceptable range. The brake pad DB10 showed high performance in recovery as 91.66 %. The temperature rise at the interface was reduced by using an air blower during a recovery test. A layer of worn out particles of pad material was deposited to the rotor face at an optimal operating temperature to ensure efficient friction mechanism. The retest was carried out under the same conditions with the existing layer of pad material after cooling to room temperature. It changed the flow behavior of particles in the surface layer during the next run. The loosely attached wear particles from the layer disintegrated and hardened by rolling abrasion mechanism. This may be a possible reason for the increase in CoF during the recovery cycle [32]. It was concluded that the addition of more amount of resin content decreased fade resistance and recovery of the brake pad material.

4.4 Friction Surface analysis after thermal load cycle

The friction surface of the brake was analyzed after fade and recovery cycle using the SEM with the magnification range of 1500x to 2600x. The SEM images are shown in Fig. 8. The microcracks observed on the worn surface on all the brake pads. The possible reason might be the degradation of organic resin binders [25]. The subsurface deformation of constituents may also be predicted as another reason for nucleating microcracks by weakened the interfacial bonding between matrix and fillers. The sizes of the microcracks increased with a decrease in

resin content. The voids and microcracks can easily form with less resin content which failed to retain the capacity of the constituents [21].

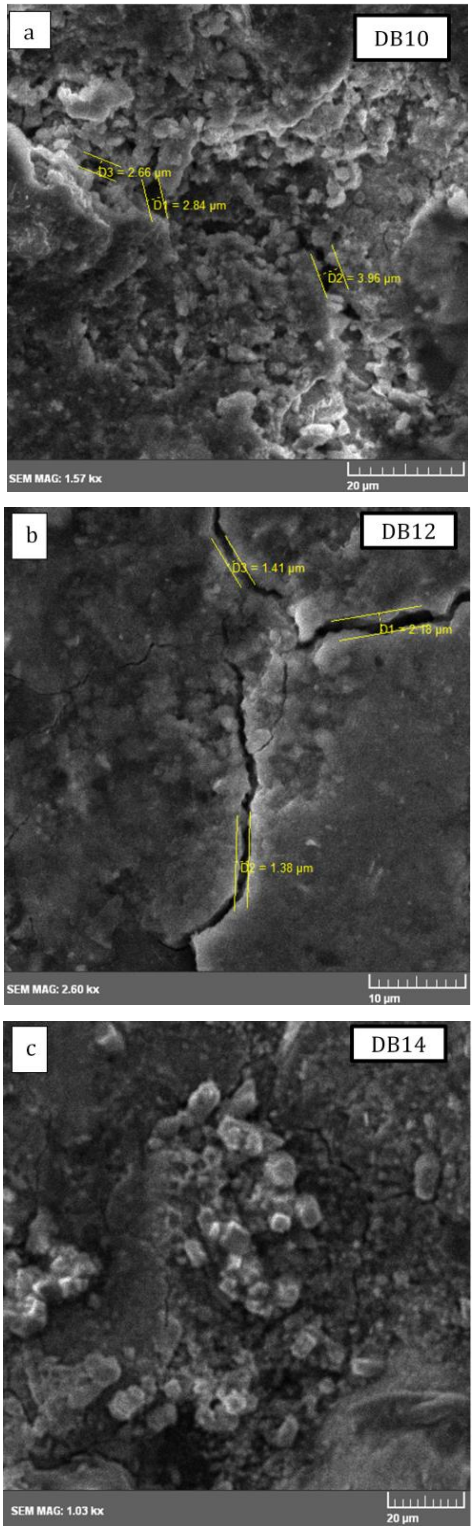

Fig. 8. SEM micrographs of (a) DB10 (b) DB12 (c) DB14 after fade and recovery cycle

In Fig. 8a, the micrograph of DB10 showed more voids and microcracks of size 2.66 µm - 3.96 µm. This may be due to insufficient wear debris backflow of the resin during the continuous braking. The Fig. 8b represented the presence of microcracks of size 1.32 µm to 2.18 µm in medium resin brake pad (DB12). In the case of DB14, as noticed in Fig. 8c, the worn surface revealed a smooth surface with less detached areas compared to DB10 and DB12. Another probable reason to wear was due to differences in the porosity of the developed friction composites. It was considered as a critical factor for heat dissipation during sliding action.

4.5 Significance of resin content on wear behaviour

The results of the wear test shown in Fig. 9a. The experiments conducted by varying the initial speed, the initial temperature of the disc and number of brake applications. The thickness loss of the brake pad measured to understand the wear of the material. It was observed that the thickness loss increased with an increase in the initial temperature of the disc for all the developed brake pads. Zhang et al. reported that the wear resistance of the materials influenced by its capacity to form transfer film on the counter surface. The growth of the tribo transfer film was based on the removal of fragments from the mating surface and lock them in the crevices of counterface asperities [33].

The composite DB14 showed the lowest wear loss as compared to DB10 and DB12 in the wear test I. The brake pad DB14 exhibited superior wear resistance in spite of its relatively poor fade resistance and thermal stability.

Wear test-I extended to the initial temperature of 300 °C (HT wear test) for 500 brake applications. The high temperature (HT) and high speed (HS) wear test results plotted in Fig. 9b. The wear test II conducted at 100 km/h and 100 °C. The relative wear loss was calculated using the equation (6) to understand the effect of temperature and rotor speed on wear loss.

$$R_{wl\ (\beta-\alpha)^\circ C} = \frac{WL_\beta}{WL_\alpha} \quad (4)$$

$R_{wl\ (\beta-\alpha)\ ^\circ C}$ = Ratio of wear loss per brake application between temperature β °C and α °C; WL_β = Wear loss per brake application at temperature β °C (β_1, β_2, and β_3 are 200, 250 and 300 °C respectively); WL_α = Wear loss per brake application at temperature α °C (α = 100 °C).

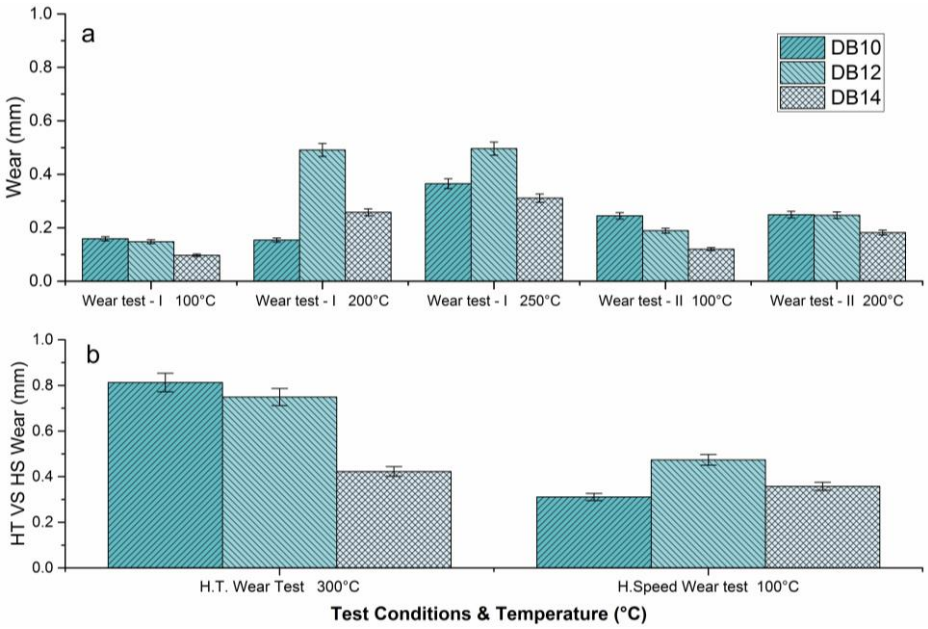

Fig. 9. (a) Wear loss of wear test I & II (b) wear loss of high temperature & high speed (100 km/h) wear test.

The ratio of wear loss $R_{wl\ (300\text{-}100)}$ for composite DB10 was observed to be 10.22 at 50 km/h and 0.3g (m/s^2) deceleration. In the case of DB12 and DB14, the wear loss ratio was noted as 10.12 and 8.72 respectively. There was no major difference in the relative wear loss of DB10 and DB12 brake pads. The DB14 exhibited slightly lower wear rate than other composites. The relative wear loss $R_{wl\ (250\text{-}100)}$ was found to vary between 2.29 and 3.35 for all the brake pads. It showed that the unexpected wear loss initiated between 250 and 300 °C. In wear test II, the ratio of wear loss $R_{wl\ (200\text{-}100)}$ found as 1.02 (DB10), 1.30 (DB12) and 1.51 (DB14). It represented that the number of applications of brake influenced the wear loss at 200 °C. The composites DB12 and DB14 offered lower wear loss than DB10. The brake pad DB10 exhibited considerable wear loss at 100 °C. This could be correlated to the lower resin content in DB10 which led to the comparatively lower interfacial strength between resin and fillers than other two composites. There were no significant changes in wear loss of DB12 and DB14 concerning a number of brake applications at 100 °C. The high porosity of the composite may be another reason to encourage the nucleation and propagation of cracks in the interface which supported the wear loss.

The ratio of wear loss of all the composites concerning temperature and speed represented in Fig. 10. The ratio of wear loss Rwl (100-50) km/h for DB10, DB12 and DB14 were calculated as 19.55, 32.09 and 36.91 respectively. Noteworthy changes observed in the ratio of wear loss after the high-speed test.

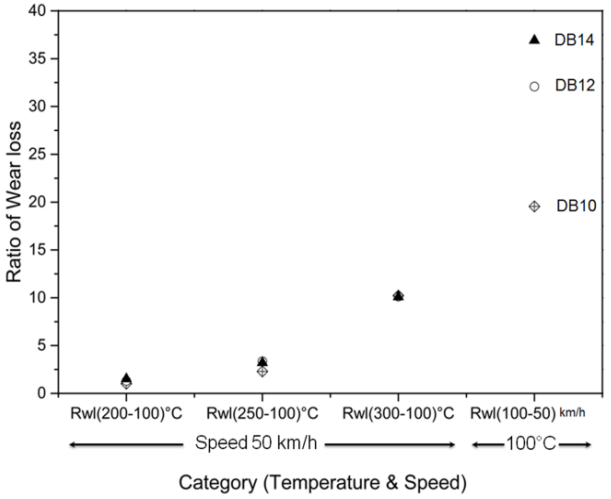

Fig. 10. The ratio of wear loss of the composites concerning temperature and speed.

The results showed that all the composites possessed wear sensitivity towards initial speed. Even though the initial temperature of rotor kept constant (100 °C), the higher (100 km/h) initial speed of the rotor resulted in drastic wear loss for the brake pad with high resin content [31]. The reason attributed to the amount of energy conversion taken place at the interface. The source of heat generation at the interface was predicted as (a) due to the initial temperature setting by the heater, (b) heat generated by braking action at high speed. It was

further predicted that the high-temperature wear process of the brake pad predominantly determined by the thermal degradation of the binder resin [10,34]. The brake pad DB14 showed lower wear loss compared to DB10 and DB12 at different temperature regimes. The composite DB14 was found to possess higher wear sensitivity (i.e., a high ratio of wear loss Rwl (100-50) km/h) with respect to the speed of the rotor than DB10 and DB12. The brake pads studied in this work are being used in the commercial passenger vehicles. The average speed of the car seldom decreases to 50 km/h or a lower value. It can be suggested that the brake pad DB10 which indicated lower wear loss at high speeds, can be a better performer.

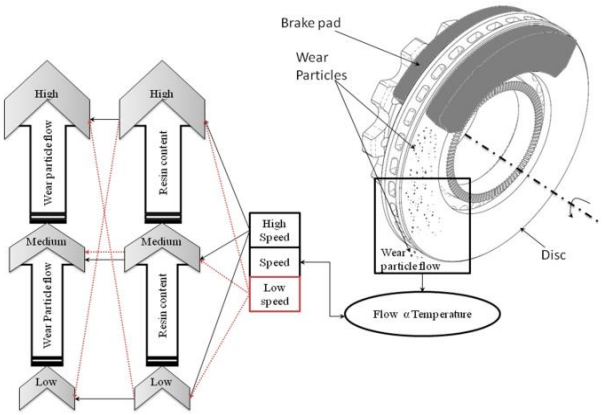

Fig. 11. Schematic diagram of wear loss of brake pads with respect to a resin content.

Figure 11 showed the schematic diagram of the wear process and the influence of speed and resin content on wear loss. The wear particle flow was generally observed to be higher for higher resin content in composites. The increment in speed also tends to increase the wear loss in composites due to higher change in kinetic energy. The wear test results at different temperature and speed regime revealed that the composite with higher resin content displayed a lower wear loss. This result prompted to study the worn surfaces of brake pads using a SEM.

4.6 Wear mechanisms at different temperature and speeds

SEM micrograph of the brake pads after wear test cycle at 100, 200 and 300 °C at 50 km/h and 100 °C at 100 km/h (HS-100 °C) shown in figure 12. The hard primary plateaus are represented as A in Fig. 12. The hard primary plateaus are the peek points of the metal fibers or other hard particles in the formulation which primarily bear the contact pressure [25]. The soft secondary plateaus represented as B are formed due to the tribo layer. The organic components were transmitted to the rotor surface after decomposition. Those relocated materials tend to back transfer to the pad due to the attraction of layers. This back transferred particles formed a layer on the pad which affects both the friction and wear [6,27,35,36]. The primary plateaus are clearly visible on the brake pads after the wear test at 100 °C with a rotor speed of 100 km/h (HS-100 °C). The pad surface covered with the transition (Secondary) layer reduced the wear of the underlying materials [15,37]. The worn surface of DB14 at 100 °C and 200 °C covered with the secondary tribo layer due to the backtransfer mechanism which is responsible for low wear. Where as at high speed (HS-100) the wear increased rapidly cause the less secondary plateau. It was predicted that there was a possibility to have increased presence of the transition layer in the composites with high resin content [21].

The flow of wear particles in composites with high resin content was higher than other brake pads. The domination of back transfer mechanism was observed to aid the formation of the transition layer. The transition layer resulted in lower wear of DB14 at low speeds and temperatures. SEM micrograph of DB14 at high speed shows that the maximum exposure of hard primary plateaus on the surface compared to DB10 and DB12 which results in high wear in DB14. The wear debris are marked as D shown in the Fig. 12. These debri's size gets reduced by the way of pressure, shear, and fragmentation.

The fragmented particles flow along the direction of sliding and piles up near the peak surface asperities and forms secondary plateaus and partly move out of the contact surfaces as wear mass loss [38]. The metal fibers of the brake pads exposed to the mating surfaces marked as C which abrade the rotor. The SEM image of the DB14 at 50 km/h and 100 °C appeared with smooth tribo layer formation. Whereas in the case of DB10 and DB12 had large wear debris which can easily be sheared off the contact surface. This evident to reduce the wear of DB14 at 100 °C. But at 100 km/h and 100 °C condition, the DB14 surface appeared with the multiple primary plateaus, pit and very high irregularity of surface.

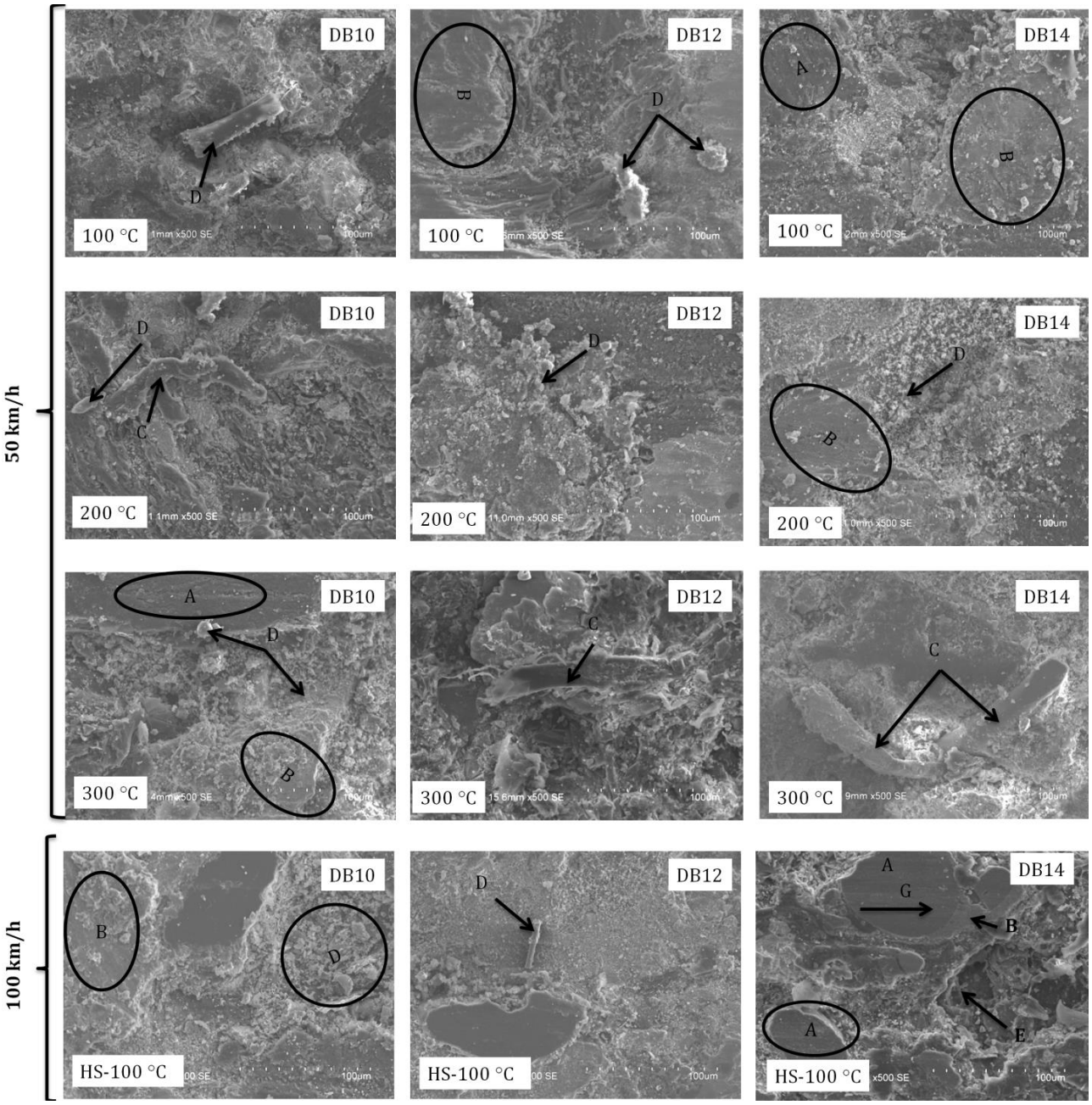

Fig. 12. SEM micrograph of DB10, DB12 and DB14 after wear test at 100, 200, 300 °C with 50 km/h, and 100 °C with 100 km/h.

Also, the primary plateaus appear with the wear track (grooves) marked as G which indicates the domination of abrasive wear caused more wear on DB14. DB12 also appeared with hard plateau had a direct contact with the rotor. The increased speed cause rapid destruction of the fragmented layer and keeps the hard patches alone to bear the load, which cause the maximum wear of DB12 at 100 km/h and 100 °C. But DB10 shows the balanced plateaus (both primary and secondary) formations with the low resin content.

5. CONCLUSIONS

a. The fraction ratio of resin showed minimal impact on the mechanical properties. The porosity, hardness and specific gravity of the brake pads decreased with the increase in resin content.

b. The thermal stability of the brake pads increased with the decreasing resin content.

c. The friction stability concerning the low pressure and speed was observed to be superior for all composites.

d. A fluctuation of friction noticed while increasing the speed and in all the composites due to the increase in interface temperature. Due to low thermal stability DB14 with a higher amount of resin degraded heavily and caused the friction mechanism change from dry lubrication system to mixed lubrication system.

e. Fade resistance of DB12 was noted to be better than DB10 and DB14. Decomposition of resin at elevated temperatures weakened the binding force and lead to the modify in real contacts at the tribo interface.

f. The brake pad DB10 performed well concerning recovery rate and moderately improved in fade rate compared to DB14.

g. Wear mechanism identified as the formation of the transition layer and nucleation of microcracks developed on the surface. The thickness of the transition layer might be increased due to more particle flow in high resin content composites.

h. The wear resistance of the DB14 is higher than the other friction composites when the speed of the rotor is 50 km/h.

i. The ratio of wear loss ($R_{wl\ (100\text{-}50)\ km/h}$) indicated that the wear rate was raised up with respect to increase in speed. The brake pad DB10 was found as a better performer at high speeds.

j. It can be concluded that the fractional ratio of resin played a significant role in friction and wear performance.

REFERENCES

[1] D. Chan, G.W. Stachowiak, *Review of automotive brake friction materials*, Proceedings of the Institution of Mechanical Engineers, Part D: Journal of Automobile Engineering, vol. 218, iss. 9, pp. 953–966, 2004, doi: 10.1243/0954407041856773

[2] J. Bijwe, *Composites as friction materials: Recent developments in non-asbestos fiber reinforced friction materials-A review*, Polymer Composites, vol. 18, iss. 3, pp. 378–396, 1997, doi: 10.1002/pc.10289

[3] S.K. Rhee, *Friction properties of a phenolic resin filled with iron and graphite - Sensitivity to load, speed and temperature*, Wear, vol. 28, iss. 2, pp. 277–281, 1974, doi: 10.1016/0043-1648(74)90169-0

[4] V.T.K. Kalaichelvan, R.V.D. Lenin, *Influence of thermal conductivity and thermal stability on the fade and recovery characteristics of non - asbestos semi - metallic disc brake pad Japanese industrial standards,* Journal of Brazilian Socity of Mechanical Sciences and Engineering, vol. 38, iss. 4, pp. 1207–1219, 2016, doi: 10.1007/s40430-015-0448-8

[5] M. Hyung, S. Jin, D. Kim, H. Jang, *Effects of ingredients on tribological characteristics of a brake lining : an experimental case study*, Wear, vol. 258, iss. 11-12, pp. 1682–1687, 2005, doi: 10.1016/j.wear.2004.11.021

[6] P.V. Gurunath, J. Bijwe, *Friction and wear studies on brake-pad materials based on newly developed resin*, Wear, vol. 263, iss. 7-12, pp. 1212–1219, 2000, doi: 10.1016/j.wear.2006.12.050

[7] B. Öztürk, S. Öztürk, *Effects of resin type and fiber length on the mechanical and tribological properties of brake friction materials*, Tribology Letters, vol. 42, iss. 3, pp. 339–350, 2011, doi: 10.1007/s11249-011-9779-5

[8] Nidhi, J. Bijwe, N. Mazumdar, *Influence of amount and modification of resin on fade and recovery behavior of non-asbestos organic (NAO) friction materials*, Tribology Letters, vol. 23, iss. 3, pp. 215–222, 2006, doi: 10.1007/s11249-006-9055-2

[9] S.J. Kim, H. Jang, *Friction and wear of friction materials containing two different phenolic resins reinforced with aramid pulp*, Tribology International, vol. 33, iss. 7, pp. 477–484, 2000, doi: 10.1016/S0301-679X(00)00087-6

[10] U.S. Hong, S.L. Jung, K.H. Cho, M.H. Cho, S.J. Kim, H. Jang, *Wear mechanism of multiphase friction materials with different phenolic resin matrices*, Wear, vol. 266, iss. 7-8, pp. 739–744, 2009, doi: 10.1016/j.wear.2008.08.008

[11] P.H.S. Tsang, M.G. Jacko, S.K. Rhee, *Comparison of Chase and inertial brake Dynamometer testing of automotive friction materials*, Wear, vol. 103, iss. 3, pp. 217–232, 1985, doi: 10.1016/0043-1648(85)90012-2

[12] K.L. Sundarkrishnaa, *Friction Material Composites Materials Prespective*, Springer, 2012.

[13] M.A.S. Balaji, K. Kalaichelvan, S. Mohanamurugan, *Effect of varying cashew dust and resin on friction material formulation : stability and sensitivity of μ to pressure , speed and temperature*, International Journal of Surface Science and Engineering, vol. 8, iss. 4, pp. 327–344, 2014, doi: 10.1504/IJSURFSE.2014.065837

[14] K. Sathickbasha, A.S. Selvakumar, M.A.S. Balaji, B.S. Rajan, *Tribo performance of Brake Friction Composite with Stainless Steel Fiber* ,in Advances in Materials and Metallurgy, Springer Singapore, 2019, doi: 10.1007/978-981-13-1780-4_17

[15] J. Bijwe, N. Majumdar, B.K. Satapathy, *Influence of modified phenolic resins on the fade and recovery behavior of friction materials*, Wear, vol. 259, pp. 1068–1078, 2005, doi: 10.1016/j.wear.2005.01.011

[16] H. Jang, K. Ko, S.J. Kim, R.H. Basch, J.W. Fash, *The effect of metal fibers on the friction performance of automotive brake friction materials*, Wear, vol. 256, iss. 3-4, pp. 406–414, 2004, doi: 10.1016/S0043-1648(03)00445-9

[17] M.A.S. Balaji, K. Kalaichelvan, *Influence of Aramid, cellulose and Acrylic fibers in NAO brake pad-effect on thermal stability and frictional characteristics*, SAE Technical Paper, vol. 5, pp. 1-8, 2013, doi: 10.4271/2013-26-0081

[18] G. Ingo, M. D'Uffizi, G. Falso, G. Bultrini, G. Padeletti, *Thermal and microchemical investigation of automotive brake pad wear residues*, Thermochimica Acta, vol. 418, iss. 1-2, pp. 61–68, 2004, doi: 10.1016/j.tca.2003.11.042

[19] F. Eddoumy, H. Kasem, H. Dhieb, J. *Gerardus, Role of constituents of friction materials on their sliding behavior between room temperature and 400 ° C*, Materials & Design, vol. 65, pp. 179–186, 2015, doi: 10.1016/j.matdes.2014.08.048

[20] E.I. Akpan, B. Wetzel, K. Friedrich, *A fully biobased tribology material based on acrylic resin and short wood fibres*, Tribology International, vol. 120, pp. 381–390, 2018, doi: 10.1016/j.triboint.2018.01.010

[21] J. Fei, H. Li, Y. Fu, L. Qi, Y. Zhang, *Effect of phenolic resin content on performance of carbon fiber reinforced paper-based friction material,* Wear, vol. 269, iss. 7-8, pp. 534–540, 2010, doi: 10.1016/j.wear.2010.05.008

[22] M. Eriksson, F. Bergman, S. Jacobson, *On the nature of tribological contact in automotive brakes*, Wear, vol. 252, iss. 1-2, pp. 26–36, 2002, doi: 10.1016/S0043-1648(01)00849-3

[23] Y. Yin, J. Bao, *Frictional performance of semimetal brake lining for automobiles*, Industrial Lubrication and Tribology, vol. 64, iss. 1, pp. 33–38, 2012, doi: 10.1108/00368791211196871

[24] P.J. Blau, *The significance and use of the friction coefficient*, Tribology International, vol. 34, iss. 9, pp. 585–591, 2001, doi: 10.1016/S0301-679X(01)00050-0

[25] M. Eriksson, S. Jacobson, *Tribological surfaces of organic brake pads*, Tribology International, vol. 33, iss. 12, pp. 817–827, 2000, doi: 10.1016/S0301-679X(00)00127-4

[26] H. Spikes, *Tribology research in the twenty-first century*, Tribology International, vol. 34, pp. 789–799, 2001, doi: 10.1016/S0301-679X(01)00079-2

[27] B. Bushan, *Introduction To Tribology,* 2nd Edition, Wiley, 2013.

[28] P. Saravanan, R. Selyanchyn, M. Watanabe, S. Fujikawa, H. Tanaka, S.M. Lyth, J. Sugimura, *Ultra-low friction of polyethylenimine / molybdenum disulfide (PEI/MoS2)15thin films in dry nitrogen atmosphere and the effect of heat treatment*, Tribology International, vol. 127, pp. 255–263, 2018, doi: 10.1016/j.triboint.2018.06.003

[29] S. Ramousse, J.W. Høj, O.T. Sørensen, *Thermal Characterisation of brake pads*, Journal of Thermal Analysis and Colorimetry, vol. 64, iss. 3, pp. 933–943, 2001, doi: 10.1023/A:101157501

[30] K. Bode, G. Ostermeyer, *A comprehensive approach for the simulation of heat and heat-induced phenomena in friction materials*, Wear, vol. 311, iss. 1-2, pp. 47–56, 2013, doi:10.1016/j.wear.2013.12.021

[31] P. Cai, Y. Wang, T. Wang, Q. Wang, *Effect of resins on thermal , mechanical and tribological properties of friction materials*, Tribology International, vol. 87, pp 1–10, 2015, doi: 10.1016/j.triboint.2015.02.007

[32] R.I. Trezona, D.N. Allsopp, I.M. Hutchings, *Transitions between two-body and three-body abrasive wear: influence of test conditions in the microscale abrasive wear test*, Wear, vol. 225–229, pp. 205–214, 1999, doi: 10.1016/S0043-1648(98)00358-5

[33] S.W. Zhang, *State-of-the-art of polymer tribology*, Tribology International, vol. 31, iss. 1-3, pp. 49–60, 1998, doi: 10.1016/S0301-679X(98)00007-3

[34] M.W. Shin, K.H. Cho, W.K. Lee, H. Jang, *Tribological Characteristics of Binder Resins for Brake Friction Materials at Elevated Temperatures*, Tribology Letters, vol. 38, iss. 2, pp. 161–168, 2010, doi: 10.1007/s11249-010-9586-4

[35] Y. Cheol, M. Hyung, S. Jin, H. Jang, *The effect of phenolic resin , potassium titanate , and CNSL on the tribological properties of brake friction materials*, Wear, vol. 264, iss. 3-4, pp. 204–210, 2008, doi:10.1016/j.wear.2007.03.004

[36] W. Österle, I. Dörfel, C. Prietzel, H. Rooch, A.L. Cristol-Bulthé, G. Degallaix, Y. Desplanques, *A comprehensive microscopic study of third body formation at the interface between a brake pad and brake disc during the final stage of a pin-on-disc test*, Wear, vol. 267, iss. 5-8, pp. 781–788, 2009, doi:10.1016/j.wear.2008.11.023

[37] M. Eriksson, *Friction and Contact Phenomena of Disc Brakes Related to Squeal,* PhD thesis, Department of Materials Science, Uppsala University, Uppsala, 2000.

[38] B. Surya Rajan, M.A. Sai Balaji, C. Velmurugan, *Correlation of field and experimental test data of wear in heavy commercial vehicle brake liners,* Friction, vol. 5, iss. 1, pp. 56–65, 2017, doi:10.1007/s40544-017-0138-x